Mat. Res. Bull. Vol. 14, pp. 109-119, 1979. Pergamon Press, Inc. Printed in the United States.

In_2O_3 : (Sn) AND SnO_2 : (F) FILMS - APPLICATION TO SOLAR ENERGY CONVERSION; PART 1 - PREPARATION AND CHARACTERIZATION

J.-C. Manifacier, L. Szepessy, J. F. Bresse, M. Perotin
Université des Sciences et Techniques du Languedoc
Centre d'Etudes d'Electronique des Solides (C.M.R.S. L.A. 21)
Place E. Bataillon, 34060 Montpellier, France

and

R. Stuck
Centre de Recherches Nucleaires
Groupe de Physique et Applications des Semiconducteurs Phase
23, rue du Loess, 67037 Strasbourg, France

(Received October 25, 1978; Refereed)

ABSTRACT

Highly conductive and transparent thin films of SnO_2 : F and In_2O_3 : Sn have been prepared using the simple pyrolitic (spray) method. The conditions of preparation are described. Results concerning electronic diffraction, dosimetry by x-ray emission (S.E.M.) and secondary ionic mass spectroscopy are reported.

Introduction

In recent years the energy crisis has accelerated research on the conversion of solar energy, and there has been a growing interest in the use of tin oxide (SnO_2) or indium oxide (In_2O_3) thin films. These layers are remarkable in that they are easily prepared in a very conductive and still highly transparent form in the visible and near infrared spectrum.

Many methods have been used to obtain SnO_2 or In_2O_3 thin films. We chose, for reasons given below, the oldest one claimed to be synthesized for the first time by McMaster (1): the gas phase hydrolysis (spray) of volatile tin or indium compound.

More elaborate methods have been used recently:

1. R. F. Sputtering (2, 3, 4) or D. C. diode sputtering (2) of mixed oxide target and reactive sputtering (5, 6) in O_2 of an indium-tin alloy target. These methods allow the fabrication of high quality films, but they have a high equipment cost and a relatively low production rate.

2. Chemical vapor deposition (CVD); the CVD process is based on the use of organometallic compound. SnO_2, SnO_2 (Sb) (7, 8), In_2O_3 (Sn) (9) films of good quality have been deposited by this method, but to adapt the process for commercial production a cheap volatile indium compound needs to be found (9).

0025-5408/79/010109-12$02.00/0

3. Other methods, oxidation of Sn films under vacuum (10, 11), flash evaporation of SnO_2 powder (12) seem to be of little commercial interest.

We chose the spraying method because it is by far the simplest and least expensive one. This method allows the deposition at relatively low temperature (substrate temperature ranging from 400 to 500°C) of highly adherent, transparent and stable layers. But because these chemical reactions are reversible, the structure and composition and, thus, the optoelectronic properties of SnO_2 or In_2O_3 films depend critically on many fabrication parameters: temperature, rate of deposition, size of the atomized particles, pressure, spraying solution, apparatus used, quality of the substrate, etc. . . . This leads to a certain scattering in the results obtained by different authors (1, 3, 14, 15, 16, 17, 18, 19). We think, anyway, that this method could be used on an industrial scale for solar energy conversion as it is already for transparent conductive coatings (Nesa coatings) and electrical resistors. On the other hand, undoped SnO_2 and In_2O_3 films are not conductive enough (they are, moreover, non-stoichiometric oxide and therefore only a metastable phase). So, to increase both the conductivity without altering the transparency and the stability of the films, extraneous impurities are introduced into the lattice: fluor for SnO_2 and tin for In_2O_3.

Experimental Procedure

The spray equipment has been described previously (13, 19). An aerosol stream containing an alcoholic solution of $SnCl_4$ or $InCl_3$ and additional dopant is sprayed through a preheating furnace whose temperature is T_1 onto a heated substrate whose temperature is T_2. Extensive care was put into devising 1) the atomizer to ensure a high degree of atomization and a finer grained surface for the deposit, and 2) the specifications of the furnace to ensure an excellent uniformity both in thickness and physical properties of the films. After trying several carrier gases: CO_2, O_2, Ar and N_2, we chose nitrogen, which is the least expensive and gives the best results.

This method of hydrolysis is based on the reversible endothermic reaction:

$$SnCl_4 + 2\ H_2O \rightleftharpoons SnO_2 + 4\ HCl$$

$$2\ InCl_3 + 3\ H_2O \rightleftharpoons In_2O_3 + 6\ HCl$$

SnO_2 and In_2O_3 thin films are not conductive enough; it is necessary to add some dopants.

For SnO_2 films, we found fluorine to be the more efficient, and we used an organo fluorine compound: trifluoroacetic acid (CF_3CO_2H) (20) or ammonium fluoride (NH_4F) in the solution. For In_2O_3 films, we used stannic chloride hydrated ($SnCl_4$, 5 H_2O). The purity of the chemical products was not found to be of critical importance, so only reagent grade chemicals were employed.

These reactions occur for temperatures higher than 300-350°C; the temperatures T_1 and T_2, as well as the solution composition, were optimized to give the best overall properties for the films (higher transparency and conductivity).

The best results were obtained with the two solutions (weight concentration).

$SnCl_4$, 5 H_2O	:	0.329	for	SnO_2 and SnO_2 : F deposits
H_2O	:	0.329 (fixed)		
CH_3CH_2OH	:	0.329 (fixed)		
NH_4F	:	0.013		Solution No. 1

and				
$InCl_3$	:	0.0817		
H_2O	:	0.4204 (fixed)	for	In_2O_3 and
CH_3CH_2OH	:	0.4204 (fixed)		In_2O_3 : Sn deposits
$SnCl_4$, 5 H_2O	:	0.0024		Solution No. 2
HCl	:	0.0751		

For both the solutions no. 1 and no. 2, the quantities of solvents (water and ethylic alcohol) were fixed. Only the concentration of the active components was varied.

As substrates we used borosilicate glass slides* for most of the measurements; for U.V. optical measurements we used quartz substrates. In the case of high substrate temperatures (T_2), some difficulties can arise with the use of standard soda lime (high alkali content) and even borosilicate (3.5 m/o NaOH and 1.15 m/o KOH) glass slides: high temperatures increase the rate of diffusion of alkali cations from the substrate into the oxide layers (7). These cations act as p-type doping agents, thus neutralizing some of the charge carriers.

In all the following studies, unless otherwise specified, the gas flow rate (nitrogen) has been chosen to be: 3 1/min and the spraying time: 3 min. The effect of the dopant concentration on the sheet resistance $R_\square$, is shown graphically in Figure 1 for the SnO_2 : F layers and in Figure 2 for the In_2O_3 : Sn layers.

In the case of doped SnO_2 : F and In_2O_3 : Sn layers the optimum substrate temperatures were found to be respectively T_2 = 500 and 506°C (cf. Figs. 1 and 2).

For Figure 2, $R_\square$ is given versus the weight concentration of $SnCl_4$, 5 H_2O, as well as the atomic ratio Sn/In in the solution.

In the following paragraph we will show that a discrepancy was found between the atomic ratio Sn/In in the solution and in the film. Extensive studies of the influence

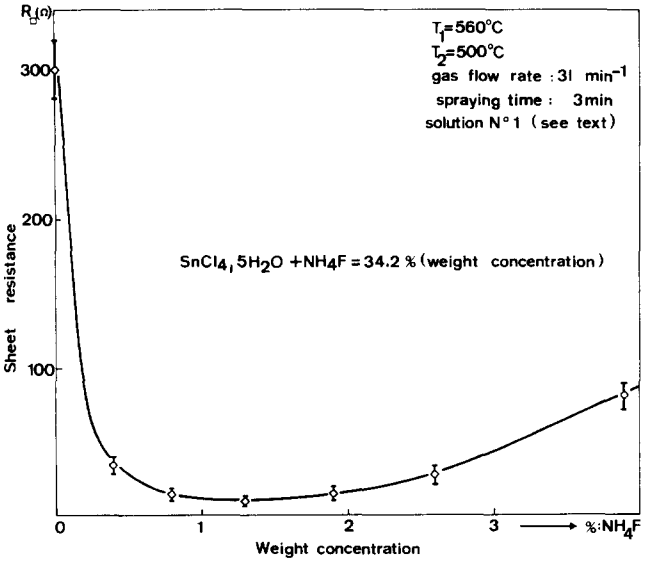

FIG. 1

Sheet resistance $R_\square$ versus NH_4F weight concentration in solution No. 1.

*Verre no. code 73201 SOVIREL, 90-92 rue Baudin, 92 Levallois-Perret, France.

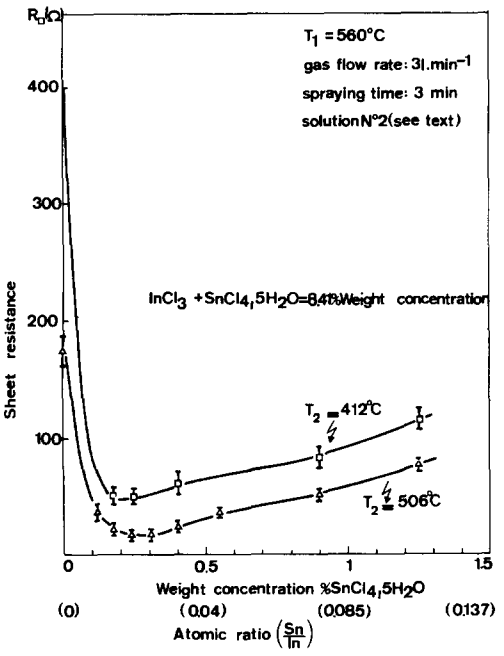

FIG. 2

Sheet resistance $R_\square$ versus $SnCl_4$, 5 H_2O weight concentration in solution No. 2. The Sn/In atomic ratio is also indicated.

on the sheet resistance of the temperature T_1 of the preheating furnace and T_2 of the substrate are given elsewhere (19). The deposition rate v_d can be very important in the spray method; v_d as high as 2000 to 4000 Å/min have been easily obtained without altering the overall qualities of the layers compared to the sputtering technique where values up to 700 Å/min have been reported (9, 10).

It should be borne in mind that all the fabrication parameters have been optimized to give the best overall characteristics for the transparency and the sheet resistance on borosilicate glasses. This optimization should correspond closely to that needed in the fabrication of spectral selective windows.

For solar cell technology, things are more complicated; a figure of merit for transparent coatings F_{TC} was first defined (21) as the ratio of the average film transmission around $\lambda = 0.5$ μm to the sheet resistance, $F_{TC} = \bar{T}/R_\square$. Recently, Haacke (22) defined a new figure of merit, $\phi_{TC} = T^{10}/R_\square$, giving more weight to the transparency and thus more adapted to solar cell technology.

Moreover, parameters such as substrate temperature (T_2) (silicon or other semiconductor compounds) during film deposition or Sn/In atomic ratio (as in the case of In_2O_3 : Sn films) can be of critical importance for the open-circuit voltage V_{oc} of the solar cell. We found recently (23) that conversion efficiency around 10% for Si (n) - In_2O_3 : Sn structures under AM1 illumination can be obtained with lower substrate temperature, T_2 = 430-450°C, and higher Sn/In atomic ratio than the ones corresponding to the minimum sheet resistance reported in Figure 2.

Characterization of the Films

Using different analytical techniques, the film structure and the chemical composition were determined. We used electron diffraction to examine the surface structure. Quantitative dosimetry was made with a JEOL type JSMU3-S.E.M. used as an x-ray analyser and an electron probe CAMECA M 546. Qualitative microanalysis was made using a secondary ion mass spectroscopy S.I.M.S. to obtain mass spectrum and concentration profiles.

First we must say that, due to the apparatus and the atomizer used, photographs with S.E.M. of the SnO_2 and In_2O_3 layers exhibit a more uniform and a finer grained surface than previously reported (19) for SnO_2 spray layers.

Electron diffraction diagram:

For all the dopant concentration (Sn or F) and substrate temperatures used, ($T_2 > 350^oC$) the deposit showed a polycrystalline structure.

SnO_2 and SnO_2 : F films:

Bulk SnO_2 and SnO crystallizes with tetragonal rutile structure according to electron diffraction observation; we observed fairly sharp rings coinciding with that of SnO_2 and SnO.

These observations are in accordance with the observation of Hecq et al. (3) and Baillou et al. (24) for SnO_2 films prepared by sputtering methods, and Kane et al. (7) for SnO_2 films prepared by a C.V.D. method. It should be noted, however, that this SnO phase is observed even if, between 300 and 1500K, SnO_2 is considerably more stable than SnO (25).

In_2O_3 and In_2O_3 : Sn films:

Bulk In_2O_3 crystallizes in a cubic b.c.c. structure.

The electron diffraction diagram coincides with In_2O_3 polycrystalline phase.

In the case of In_2O_3 : Sn, no SnO_2 phase was detected (for the Sn dopant concentration used), implying that Sn replaces In substantially in the In_2O_3 structure. These results are in accordance with the ones of Vossen (2), Bosnell and Waghorne (4), and Heq et al. (3) who used sputtering methods, and Köstlin (26) who used a similar pyrolitic method.

Köstlin et al. (26) observed that no SnO_2 phase is observed at concentration below 60 at. % Sn, and Hecq et al. (3) observed that for concentration below 35 at. %In, the presence of SnO, SnO_2 and In_2O_3 : Sn films prepared using sputtering methods.

A [111] privileged orientation was found, as is usually reported (26) in the case of films prepared using a spray method. Vossen (2) reports a [100] direction perpendicular to the substrate, Fraser and Cook (21) and Hecq et al. (3) a [111] direction perpendicular to the substrate for In_2O_3 : Sn films prepared using sputtering methods.

Electron probe microanalysis:

These measurements were made using an electron probe or a S.E.M. We carried out Sn and F dosimetry in SnO_2 : F layers as well as In and Sn dosimetry in In_2O_3 : Sn layers.

This analysis is valid for relative comparison only as the In_2O_3 and SnO_2 layers have a thickness less than the electron penetration (12). We chose layers of approximately the same thickness so the intensity ratio In $L\alpha$/Sn $L\alpha$ of the x-ray emission is assumed to correspond closely to atomic ratio.

The same assumption was made by different authors using x-ray fluorescence analysis (3, 8, 21). For all the measurements made, the concentration of the elements analysed was found to be nearly constant along the sample. (See discussion.)

SnO_2 : F layers:

Difficulties arise in this case due to the light atomic mass of F leading to a very poor x-ray emission yield.

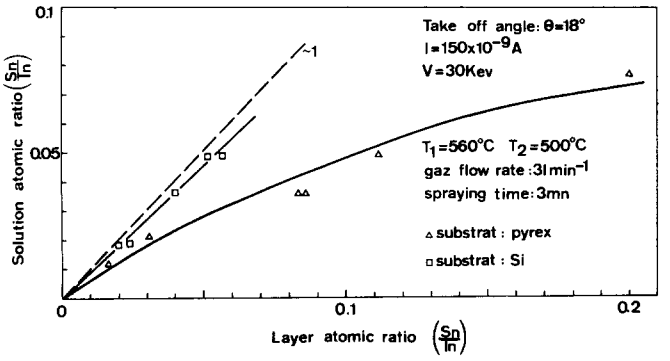

FIG. 3

Sn/In atomic ratio in the In_2O_3:Sn layers versus Sn/In atomic ratio in the solution, as determined by x-ray analysis.

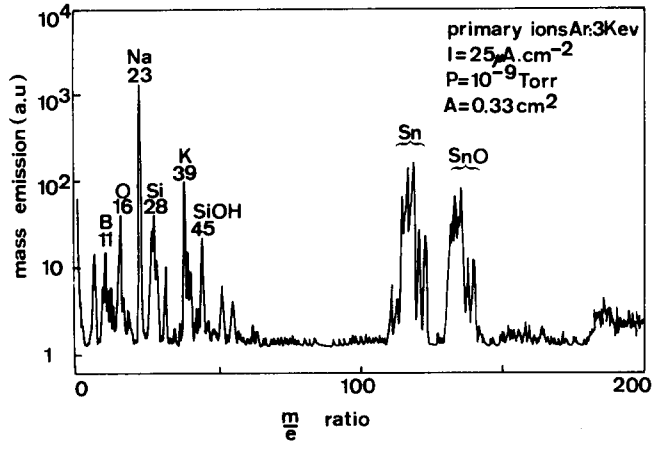

FIG. 4

Dynamic positive secondary ion mass spectrum on an SnO_2 : F layer (borosilicate glass substrate).

For layers of the lowest resistivity (cf. Fig. 1 and Table 1) the NH_4F weight concentration in the solution 1 is around 1.3 % corresponding to an atomic ratio F/Sn ~ 0.38, while the F/Sn atomic ratio in the layer is found to be less than a few per cent. This result is not surprising as fluorine compounds decompose at these temperatures (probably HF under gaseous form).

In_2O_3 : Sn layers:

The Sn/In ratio measured by x-ray analysis is plotted as a function of the Sn/In ratio in the solution no. 2 in Figure 3. We used borosilicate glass slides or silicon substrates.

In the case of silicon substrates, the concentration of Sn incorporated in the sprayed solution is practically identical with that of the film as it was reported by Köstlin et al. (26) and Kane and Schweitzer (9). In the case of borosilicate glass substrates, an important discrepancy is observed (cf. Fig. 3). This discrepancy is not well understood at this time.

S.I.M.S. measurements:

The secondary ion mass spectrometry measurements were performed in a Balzers apparatus, where the current density of the primary 3 Kev argon ions beam was varied between 50 and 0.05 $\mu A/cm^2$. Since the escape depth of these secondary ions is of the order of 10-20Å, the analysis is localized in a shallow depth; moreover, the surface of the substrate being continuously eroded during the bombardment, it is

also possible to perform depth profiling by monitoring the selected masses versus time. Unfortunately, no information on chemical bonding can be obtained by this method, since most of the bonds are broken by the irradiation.

All experiments were performed in high vacuum (10^{-9} Torr) in order to avoid the fast build-up of contamination layer on the analysed surface.

SnO_2 : F films on borosilicate glass slide:

Positive and negative secondary ion mass spectra are shown on Figures 4 and 5 respectively for a typical SnO_2 : F layer prepared on a borosilicate glass substrate. These spectra were taken for a depth of about 600 Å inside the SnO_2 : F layer whose thickness was t = 4200 Å.

An important contamination by bore, sodium, aluminium, potassium, silicium and subsequent oxides of these elements was noted.

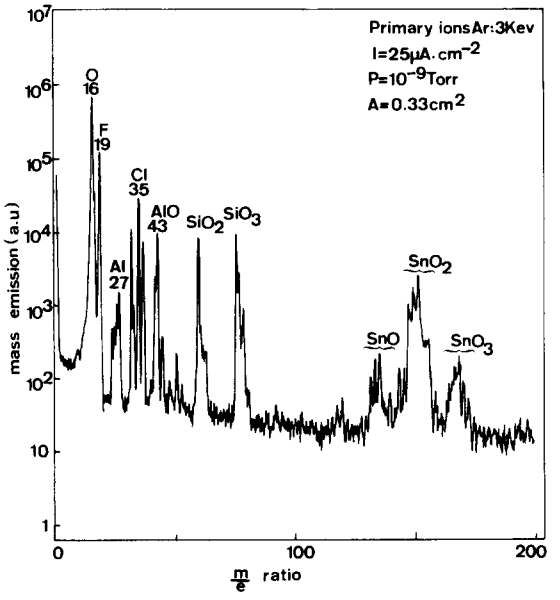

FIG. 5

Dynamic negative secondary ion mass spectrum on an SnO_2 : F layer (borosilicate glass substrate).

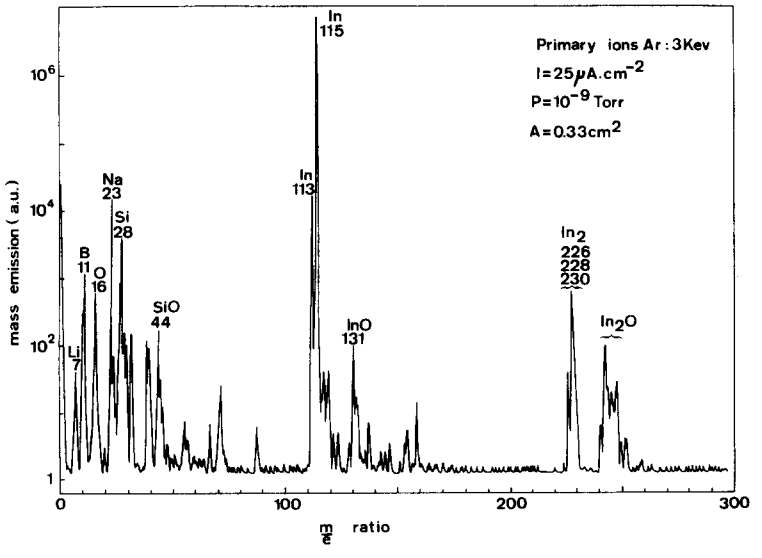

FIG. 6

Dynamic positive secondary ion mass spectrum on an In_2O_3 : Sn layer (borosilicate glass substrate).

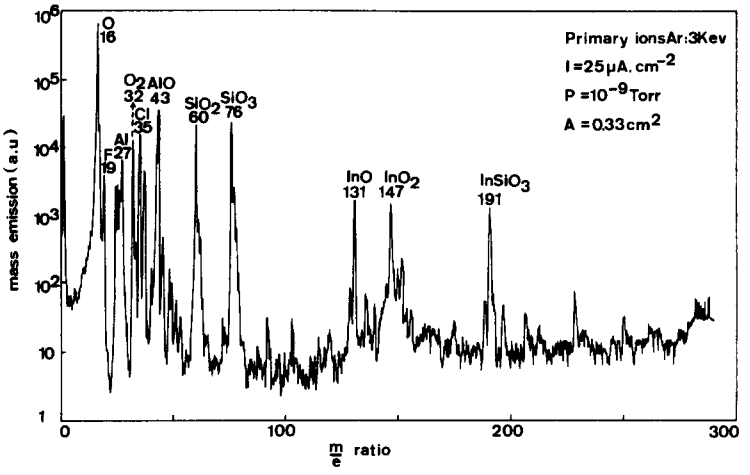

FIG. 7

Dynamic negative secondary ion mass spectrum on an In_2O_3 : Sn layer (borosilicate glass substrate).

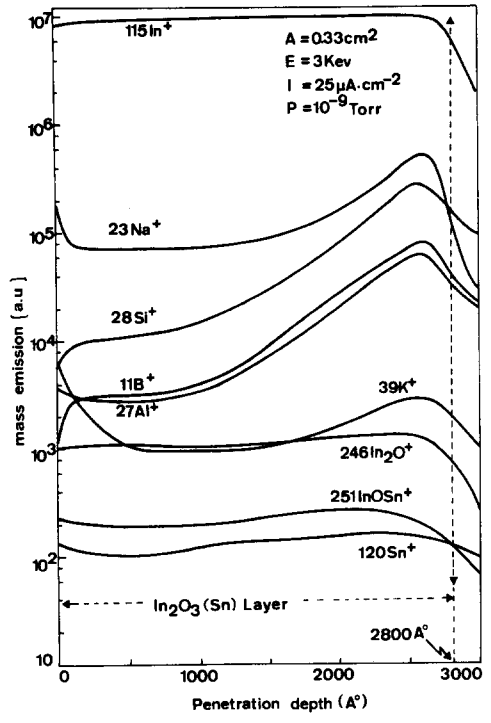

FIG. 8

Depth profiling for an In_2O_3-Sn layer - positive ion mass spectra (borosilicate glass substrate).

These impurities do not come from the solution used, but from the pyrex substrate used as is shown below by S.I.M.S. for SnO_2 : F layers on silicon substrates. In this case, the level of these impurities was found to be two or three orders of magnitude lower. (The borosilicate slides used were composed of SiO_2, Al_2O_3, B_2O_3, NaOH and KOH.)

It should be noted that even for lower substrate temperature, $T_2 \sim 430\text{-}450^{\circ}C$, the rate of diffusion of alkali cations from the pyrex substrate into the oxide layer is still very important.

In_2O_3 : Sn films on borosilicate glass slide:

Positive and negative secondary ion mass spectra are shown in Figures 6 and 7 respectively for a typical In_2O_3 : F layer under similar experimental conditions.

The same impurities appear in these spectra, but as no calibration was performed for these measurements only qualitative comparisons can be made. Examples of profiling by S.I.M.S. for the same In_2O_3 : Sn layer obtained by monitoring the intensity of appropriate masses for a large area under continuous ion bombardment are shown in Figures 8 and 9.

The accumulation at the interface of alkali ions and silicon can be noted, the borosilicate glass substrate acting as a diffusion sourse for these elements.

The thickness of the layer (t = 2800 Å in this case) determined by using both optical and mechanical Talystep measurements was used to calibrate the penetration

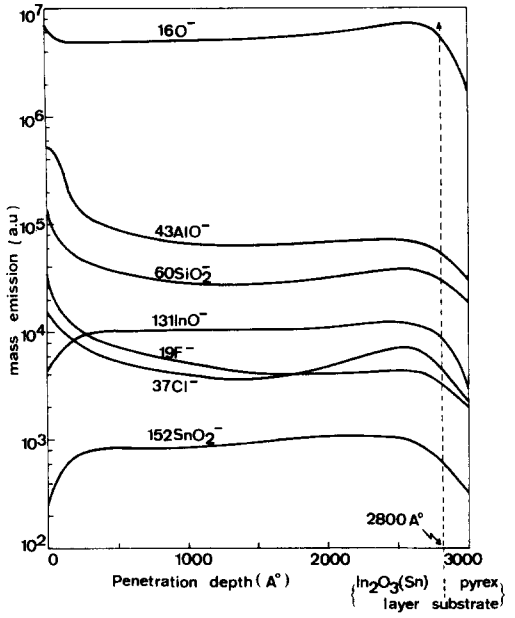

FIG. 9

Depth profiling for an In_2O_3-Sn layer - negative ion mass spectra (borosilicate glass substrate).

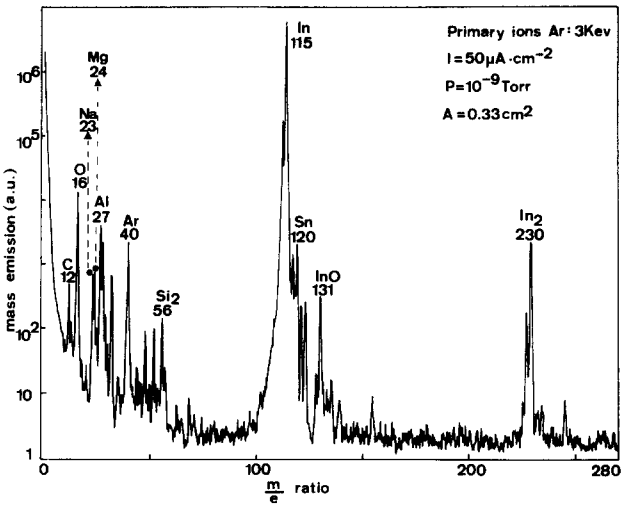

FIG. 10

Dynamic positive secondary ion mass spectrum on an In_2O_3 : Sn layer (silicon substrate).

depth axis.

In_2O_3 : Sn film on silicon substrate:

These spectra are shown in Figures 10 and 11 under the same experimental conditions except for the current density of the primary argon ion beam, which was chosen equal to 50 $\mu A/cm^2$.

From Figures 10 and 11, by comparison with Figures 6 and 7, we can deduce that most of the peaks associated with alkali impurities and subsequent oxides are much more weak (nearly two orders of magnitude for Na^+ and even more for B^+).

Discussion

The polycrystalline nature of the films results in a granular structure as can be seen in photographs with S.E.M. Special care was taken in devising the apparatus of preparation so reducing the size of the crystallites to less than 0.1 μm. We observed some scattering in the electron probe microanalysis results.

Variation of about 10-15% in x-ray emission for Sn and In was measured along the samples, and this variation, for the method of preparation used, does not seem to be related to a corresponding inhomogeneity for these elements in the layers. It is plausible that this is a consequence of the smooth structure of the films.

The important contamination of alkali elements (B, Na, K . . .) which were shown to diffuse from the glass substrate should be of no critical importance for highly doped samples. This contamination could explain the lack of reliability reported by many authors in the variation of the resistivity after heating cycles for undoped layers.

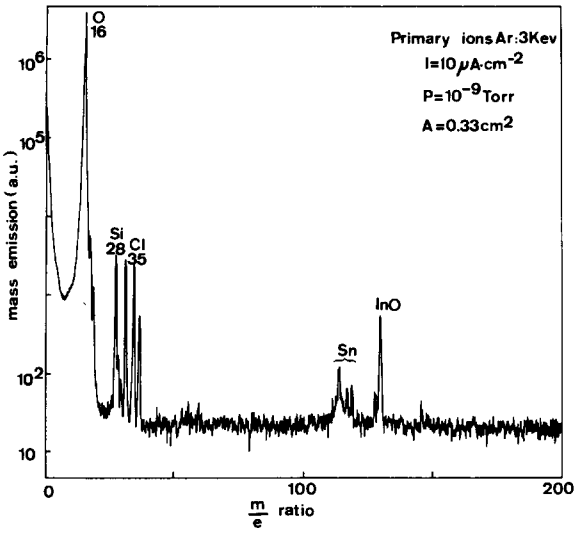

FIG. 11

Dynamic negative secondary ion mass spectrum on an In_2O_3 : Sn layer (silicon substrate).

Conclusion

The spraying method used is a very unsophisticated method, allowing the preparation in a few minutes of stable, highly resistant, transparent and conductive SnO_2, In_2O_3 or mixed compounds layers. This method should be effective for the preparation of such films, on an industrial scale, in solar energy conversion systems (solar cells and flate plate collectors technologies).

For these special purposes, the (small) scattering observed in the properties of these layers should be of no practical importance.

Acknowledgments

The authors would like to thank Professors M. Savelli, J. P. Fillard and P. Siffert for their support.

References

1. Libbey-Owens-Ford Glass Co., and H. A. McMaster, Brit. Pat. 632, 256 (1942).
2. J. L. Vossen, RCA Rev. 32, 289 (1971).
3. M. Hecq, A. Dubois and J. Van Cakenberghe, Thin Solid Films 18, 117 (1973).
4. J. R. Bosnell and R. Waghorne, Thin Solid Films 15, 141 (1973).
5. F. Buigez, G. Bomchill, S. Galzin and A. Monfret, Colloque Microélectronique, p. 146, Montpellier, France, 16-19 Nov. (1976).
6. E. Giani and R. Kelly, J. Electrochem. Soc.: Solid State Science and Technology 121, 394 (1974).
7. J. Kane, H. P. Schweitzer and W. Kern, J. Electrochem. Soc. 122, 1144 (1975).
8. J. Kane, H. P. Schweitzer and W. Kern, J. Electrochem. Soc. 123, 270 (1976).
9. J. Kane and H. P. Schweitzer, Thin Solid Films 29, 155 (1975).

10. M. Watanabe, Jap. J. Appl. Phys. 9, 1551 (1970).

11. T. Nishino and Y. Hamakawa, Jap. J. Appl. Phys. 9, 1085 (1970).

12. J.-C. Manifacier, M. De Murcia and J. P. Fillard, Thin Solid Films 41, 127 (1977).

13. K. Ishiguro, T. Sasaki, T. Arai and I. Imai, J. Phys. Soc. Jap. 13, 296 (1958).

14. A. Ya. Kuznetsov, Sov. Phys. - Solid State 2, 30 (1960).

15. F. Van der Maesen and C. H. Witmer, Comptes Rendus du 7^{O} Congres International, Physique des Semiconducteurs, dunod, 1211, Paris (1964).

16. V. K. Miloslavskii, Optics and Spectroscopy 7, 154 (1959).

17. A. R. Peaker and B. Horsley, Rev. Sci. Instrum. 42, 1825 (1971).

18. R. Groth, Phys. Stat. Sol. 14, 69 (1966).

19. J.-C. Manifacier, M. De Murcia and J. P. Fillard, Mat. Res. Bull. 10, 1215 (1975).

20. A. Ya. Kuznetsov, A. V. Kruglova and B. P. Kryshanovskii, J. Appl. Chem. of the USSR 32, 1186 (1959).

21. D. B. Fraser and H. D. Cook, J. Electrochem. Soc. 119, 1368 (1972).

22. G. Haacke, J. Appl. Phys. 47, 4086 (1976).

23. J.-C. Manifacier, L. Szepessy, Appl. Phys. Lett. 31, 459 (1977).

24. J. Baillou, P. Pugnet, J. Deforges, S. Durand and G. Batailler, Rev. Phys. Appl. 3, 78 (1968).

25. C. A. Vincent, J. Electrochem. Soc. 119, 515 (1972).

26. H. Köstlin, R. Jost and W. Lems, Phys. Stat. Sol. 29a, 87 (1975).